Published in final edited form as:

Cerebellum. 2018 August ; 17(4): 392–403. doi:10.1007/s12311-014-0571-6.

Bergmann glia are patterned into topographic molecular zones in the developing and adult mouse cerebellum

Stacey L. Reeber, **Marife K. V. Arancillo**, and **Roy V. Sillitoe***

Department of Pathology & Immunology, Department of Neuroscience, Baylor College of Medicine, Jan and Dan Duncan Neurological Research Institute of Texas Children's Hospital, 1250 Moursund Street, Suite 1325, Houston, Texas 77030, USA

Abstract

Cerebellar circuits are patterned into an array of topographic parasagittal domains called zones. Zones are best revealed by gene expression, circuit anatomy, and cellular degeneration patterns. Thus far, the study of zones has been focused heavily on how neurons are organized. Because of this, detailed neuronal patterning maps have been established for Purkinje cells, granule cells, Golgi cells, unipolar brush cells, and also for the terminal field organization of climbing fiber and mossy fiber afferents. In comparison, however, it remains poorly understood if glial cells are also organized into zones. We have identified an *Npy-Gfp* BAC transgenic mouse line (*Tau-Sapphire Green fluorescent protein* (*Gfp*) is under the control of the *neuropeptide Y* (*Npy*) gene regulatory elements) that can be used to label Bergmann glial cells with Golgi-like resolution. In these adult transgenic mice we found that *Npy-Gfp* expression was localized to Bergmann glia mainly in lobules VI/VII and IX/X. Using double immunofluorescence, we show that in these lobules, *Npy-Gfp* expression in the Bergmann glia overlaps with the pattern of the small heat shock protein HSP25, a Purkinje cell marker for zones located in lobules VI/VII and IX/X. Developmental analysis starting from the day of birth showed that HSP25 and *Npy-Gfp* expression follow a similar program of spatial and temporal patterning. However, loss of Npy signaling did not alter the patterning of Purkinje cell zones. We conclude that Bergmann glial cells are zonally organized and their patterns are restricted by boundaries that also confine cerebellar neurons into a topographic circuit map.

Keywords

topography; circuitry; connectivity; patterning; Purkinje cells; glial cells

*Address correspondence to: Dr. Roy V. Sillitoe, Tel: 832-824-8913, Fax: 832-825-1251, sillitoe@bcm.edu.

Contributions: SLR and RVS designed the experiments. SLR, MKVA and RVS performed the experiments. SLR, MKVA and RVS wrote the paper.

Conflicts of Interest: We have nothing to disclose.

The content is solely the responsibility of the authors and does not necessarily represent the official views of the National Center For Research Resources or the National Institutes of Health.

Introduction

Brain circuits are patterned into spatial connectivity maps that control animal behavior. For example, the cerebral cortex contains ocular dominance columns that encode visual cues and barrels that participate in somatosensation, the basal ganglia contain patches and matrices that control movement, the olfactory bulb contains sensory maps for odor discrimination, and the cerebellum contains zonal "stripe" maps that may be essential for controlling motor behavior (1–3). The compartmental features of each map are best understood by neuronal gene expression and connectivity. Yet, we have a poor understanding of whether glial cells are patterned into these brain maps. This study addresses two questions: 1) Are glial cells patterned into topographic cerebellar maps? 2) If glial cells are patterned in cerebellar maps, how does their organization relate to neuronal zone patterning? We have used bacterial artificial chromosome (BAC) transgenic mice that express *Tau-Sapphire Green fluorescent protein* (*Gfp*) under the control of the *neuropeptide Y* (*Npy*) regulatory elements (4) to genetically dissect the zonal patterning of Bergmann glia in the developing and adult cerebellum.

Glial cells constitute at least half of all cells in the nervous system, and they are required for maintaining synapses and controlling synaptic plasticity during brain function (5–7). Golgi type II epithelial cells, or Bergmann glia, are specialized astrocytes that play multiple roles during the development and function of the cerebellum (8). During the first two postnatal weeks they provide structural support for guiding the migration of newly differentiated granule cells from the external granular layer to the internal granular layer (9). These morphogenetic functions of the Bergmann glia ultimately have a critical influence on foliation (10, 11). Bergmann glia also play a role in the elaboration of Purkinje cell dendrites by providing a scaffold for dendrite extension (8). Thus, in the developing cerebellum glia are essential for generating neuronal architecture and for specifying neuronal position, two processes that establish circuit connectivity. The influence of Bergmann glial cells during circuit construction is followed by their critical impact on the function of adult networks, where they are essential for optimizing the structural and functional integrity of circuits for proper synaptic transmission (12). Given that cerebellar neurons form highly organized zonal circuits (1, 3), and because the neurons in each zone are normally associated with glial cells, we hypothesized that in order for Bergmann glia to influence cerebellar function they might also follow, and perhaps be constraint by, the spatial and temporal patterning of the zones.

To test our hypothesis we used transgenic reporter expression and immunohistochemistry to map the pattern of *Npy-Gfp* in Bergmann glial cells of the developing and adult mouse cerebellum. Our study demonstrates for the first time that Bergmann glia are zonally patterned in the normal cerebellum. We found that the pattern of *Npy-Gfp* expression in Bergmann glia overlaps with the pattern of HSP25 in Purkinje cell zones. We also found that the neuronal pattern of HSP25 and the glial pattern of *Npy-Gfp* followed the same developmental trajectory, as the two patterns exhibited a similar organization at all postnatal ages studied. These results suggest that neurons and glial cells are intimately linked by cerebellar zone topography. The data also indicate that in the developing cerebellum, the timetables of neuronal and glial patterning may be coordinated for establishing the

functional cellular interactions that control circuit function and motor behavior. However, genetic deletion of the *Npy* gene did not alter Purkinje cell zonal topography, indicating that Npy signaling in Bergmann glial zones does not instruct the compartmental patterning of cerebellar circuitry.

Materials and Methods

Mice

All animal studies were carried out under an approved IACUC animal protocol according to the institutional guidelines at Albert Einstein College of Medicine (Bronx, NY) and at Baylor College of Medicine (Houston, TX). Female and male *neuropeptide Y* (*Npy-Gfp*) transgenic mice (2, 4, 13) were obtained from The Jackson Laboratory, (Bar Harbor, ME) and maintained in our colony on a C57BL/6J background. The *Npy-Gfp* mice were generated using bacterial artificial chromosome technology (BAC) to insert a *Tau-Sapphire* fusion reporter cassette downstream of the *Npy* gene's regulatory elements (4). The modified and purified BAC DNA was injected by standard pronuclear injection (4). Homozygous Npy^{LacZ} knock-in mice were purchased as homozygote breeder pairs from the Jackson Laboratory and thereafter maintained in our colony (14). We performed homozygous to homozygous crosses to generate mutants ($Npy^{LacZ/LacZ}$) and we analyzed heterozygotes ($Npy^{LacZ/+}$) from backcrosses to C57BL/6J. All mating's were timed and based on the presence of a vaginal plug. Noon on the day a vaginal plug was detected was considered embryonic day (E) 0.5. The day of birth was designated as postnatal day (P) 0, and mice that were P28 or older were considered mature. Male and female *Npy-Gfp* mice were analyzed at postnatal day (P) 0 ($n = 5$), P2/3 ($n = 5$), P5 ($n = 4$), P10 ($n = 6$), and as mature adults ($n = 16$). Mice carrying the *Npy-Gfp* allele were identified by genotyping using a standard PCR protocol with primers designed to detect the *Gfp* cassette (GFP 5′sense: CTGGTCGAGCTGGACGGCGACG, GFP 3′antisense: CACGAACTCCAGCAGGACCATG). The expected band size is ~ 600 bp when run and visualized on a 2% agarose gel made with ethidium bromide. The Npy^{LacZ} mice were genotyped by incubating a 2 mm piece of tail clip in X-gal reaction buffer for 4 – 8 hours at 37 degrees (see below). We analyzed male and female Npy^{LacZ} mice at P28 or older ($n = 9$ mutants and $n = 6$ controls).

Immunohistochemistry

Mice were anesthetized with avertin. Once all reflexes were abolished (e.g. lack of blink and toe pinch reflexes) the blood was flushed through the heart by perfusing with 0.1M phosphate buffered saline (PBS; pH7.2). The tissue was then fixed by perfusing with 4% paraformaldehyde (4% PFA) diluted in PBS. The brains were then postfixed for 24–48 hours in 4% PFA and then cryoprotected in buffered sucrose solutions (15% and then 30% diluted in PBS). Serial 40 μm thick coronal sections were cut on a cryostat and collected as free-floating sections in PBS. Immunohistochemistry was carried out as described previously (15, 16). Briefly, the tissue sections were washed thoroughly, blocked with 10% normal goat serum (NGS; Sigma, St. Louis MO, USA) for 1 hour at room temperature and then incubated in 0.1M PBS containing 10% NGS, 0.1% Tween-20 and the primary antibodies (see below) for 16–18 hours at room temperature. The tissue sections were then washed

three times in PBS and incubated in secondary antibodies (see below) for 2 hours at room temperature. Then the tissue was rinsed again and immunoreactivity revealed as described below.

Rabbit polyclonal anti-HSP25 (1:500; Catalogue # SPA-801) was purchased from StressGen (Victoria, BC, Canada) and its expression in tissue revealed a pattern identical to what has previously been reported in the mouse cerebellum (17). Rabbit anti-GFP (1:1000) was purchased from Molecular Probes (Invitrogen; Carlsbad, CA). Chicken anti-GFP (1:2000) was purchased from Abcam (Cambridge, MA). Glial Fibrillary Acidic Protein (GFAP; 1:500; Cat. # AB5804) and tenascin (1:500; Cat. # AB19011) were purchased from Chemicon (Millipore, Temecula, CA, USA) and we used them to mark Bergmann glia in the adult cerebellum (18, 19).

We visualized immunoreactive complexes either using diaminobenzidine (DAB; 0.5 mg/ml; Sigma, St. Louis, MO, USA) or fluorescence. For the DAB reaction we used horseradish peroxidase (HRP) conjugated goat anti-rabbit (diluted 1:200 in PBS; DAKO, Carpinteria, CA, USA) antibodies to bind the primary antibodies. Staining for fluorescent immunohistochemistry was carried out using Alexa 488- and 555-conjugated immunoglobulins (Molecular Probes Inc., Eugene, OR, USA), both diluted 1:1500. Tissues sections were coverslipped using FLUORO-GEL with Tris buffer (Electron Microscopy Sciences, Hatfield, PA). We tested the specificity of the secondary antibodies by processing the tissue sections in the absence of primary antibodies. No signal was detected in such control experiments indicating that the staining we observed was not due to non-specific signals from the Alexa or HRP conjugated antibodies (data not shown).

X-gal staining to detect β-galactosidase

We performed the X-gal staining as previously described (20). The whole brain was immersed in the reaction buffer until the intense blue reaction product was visible.

Golgi-Cox staining

We performed the Golgi-Cox staining (21) with a modified procedure using the FD Rapid GolgiStain Kit (FD Neurotechnologies, Inc). The main difference is that before staining we flushed the blood from the brain by perfusing the mice with PBS for 2 minutes before quickly removing the brain from the skull. The tissue sections were cut at 80 μm on a cryostat and processed as described by the manufacturer using a free-floating approach ($n = 6$). The stained neurons were imaged as described below.

Microscopy and data analysis

Photomicrographs of tissue sections were captured using Leica DFC 360 FX (fluorescence) and DFC 490 (DAB reacted tissue and Golgi-Cox staining) cameras mounted on a Leica DM5500 microscope. Images of the tissue sections were acquired and analyzed using Leica Application Suite and Leica Application Suite FX software supplemented with a deconvolution module. For deconvolution, stacks of 10–20 sections in the z-axis were collected every 0.2–0.5 μm. The z stack images were deconvolved (~10 iterations) and then analyzed as compressed projections or as individual slices. Photomicrographs of

wholemount X-gal stained brains were captured with a Leica MZ16 FA stereomicroscope mounted with a Leica DFC3000 FX camera running Leica LAS software supplemented with the Leica Montage module. After wholemount staining, some cerebella were cryoprotected and then cut frozen at 40μm. The tissue sections were mounted and then imaged using a Zeiss AxioCam MRc5 camera mounted on a Zeiss Axio Imager.M2 microscope. High-resolution z-stacks were acquired with a constant inter-stack interval and select "slices" were segmented out and analyzed using the Zeiss ZEN software (2012 edition). The raw data was imported into Adobe Photoshop version CS5 and corrected for brightness and contrast only. The schematics were drawn in Adobe Illustrator version CS5.

Statistical analysis

The cerebellar vermis is comprised of ten anatomically distinct lobules (22, 23). Gene expression and functional connectivity can be used to organize the lobules into four broad transverse domains (24, 25) referred to from anterior to posterior as: the anterior (lobules I–V), central (lobules VI and VII), posterior (lobules VIII and anterior IX), and nodular domain (lobules posterior IX and X). The number of labeled Bergmann glia in lobules I–V, VI–VII, VIII–IX, and IX–X of *Npy-Gfp* mice were computed based on equally spaced 40 μm sections (sampled from within ~200–300 μm of the midline, with the limits chosen to ensure that counts of Bergmann glia that were positive for GFP were restricted to the vermis, and not the paravermis or hemispheres. 6 tissue sections per animal were used for the analysis ($n = 4$ animals analyzed). The number of GFP positive profiles, which we could clearly identify as Bergmann glia based on their distinct palisade morphology (their processes extend to the pial surface) and the location of their cell bodies within the Purkinje cell layer, were counted for each lobule and computed per transverse domain. The sum of the number of Bergmann glia for each domain was calculated and the mean for each domain was used to calculate the SEM. The p value (considered significant only if <0.05) was acquired using a one-way ANOVA test (GraphPad Prism) to compare the differences in the number of *Npy-Gfp* expressing Bergmann glia that reside in each of the four transverse domains.

Results

Npy-Gfp transgene expression marks cerebellar neurons, afferent projections, and Bergmann glial cells

Npy is expressed in neuronal somata and afferent projections throughout the brain (4, 13, 26–29). In the cerebellum, Npy is best known for its expression in climbing fiber projections (2, 13, 30, 31) (Fig. 1A). Using an *Npy-Gfp* transgene (13), we detected reporter expression in other cerebellar populations including Purkinje cells (Fig. 1A), inhibitory interneurons (Fig. 1C), and mossy fibers (Fig. 1D). Consistent with the endogenous expression of Npy, which has been revealed by large-scale gene expression analysis (26, 32), we also observed *Npy-Gfp* expression in developing and adult Bergmann glia (Fig. 1B). At E15, *Npy-Gfp* expression was restricted to small clusters of radial glia, which are the embryonic precursors that give rise Bergmann glial cells of the adult cerebellum (Fig. 2A, white asterisks and 2B). We identified the radial glia anatomically by their long radial fibers (white arrowheads Fig. 2B) with endfeet that project to the ventricular surface (white arrow Fig. 2B). It should be

noted however that even though the marked cells had these glial features, a portion of them could be immature neurons. But based on their mature anatomical features, we could positively identify adult *Npy-Gfp* labeled Bergmann glial cells based on their unique morphology and their location within the Purkinje cell layer (33) (Fig. 1B, Fig. 3A). *Npy-Gfp* labels both the primary ascending shaft and the laterally extending processes of Bergmann glial cells with "Golgi-like" resolution (Fig. 1B, Fig. 3A). Note that similar to the actual Golgi-Cox staining, *Npy-Gfp* fills entire cells revealing the exquisite structure of the Bergmann glia in the Purkinje cell layer. To confirm the identity of labeled cells as Bergmann glia, we double labeled tissue sections with anti-GFP and either anti-GFAP or anti-tenascin. In the rodent cerebellum, GFAP (18) and tenascin (19) are heavily expressed in adult Bergmann glia. GFAP and tenascin were co-labeled with *Npy-Gfp* in the ascending processes that extend from the somata in the Purkinje cell layer all the way to the pial surface (Fig. 3B, C).

Bergmann glial cells that express the *Npy-Gfp* transgene are restricted to specific lobules

GFP marked Bergmann glia were not distributed equally throughout the anterior-posterior axis of the adult cerebellum (Figure 3D–F and schematic; $n = 6$). Instead, we found significantly higher numbers of marked cells in lobules VI–VII and lobules IX (caudal)-X (mean (VI–VII) = 21 cells ± 9; mean (IX–X) = 16 cells ± 10; Fig. 3D, F, G) compared to the lobules I–V and VIII–IX (rostral) (mean (I–V) = 5 cells ± 5; mean (VIII–IX) = 6 cells ± 4; ANOVA: $F(3,40) = 12.24$, $P<0.0001$; Tukey HSD post hoc test: I–V vs. VI–VII and IX–X, $p<0.0001$ (****); I–V vs. VIII–IX = not significant; VIII–IX vs. VI–VII and IX–X, $p<0.05$ (*); VI–VII vs. IX–X, not significant; Fig. 3D, E, G). These data, together with previous knowledge that subsets of lobules have distinct cellular lineages, developmental timetables, and functional circuitries (25), suggested the possibility that Bergmann glia may be patterned and follow the well known "zonal" architecture of the cerebellum (1). Therefore, we next determined whether the restricted expression in the anterior-posterior axis was related to zones, which partition the medial-lateral axis.

Npy-Gfp transgene expression reveals a zonal pattern in cerebellar Bergmann glia

The unequal distribution of *Npy-Gfp* labeled Bergmann glia across the ten lobules, with the highest numbers in lobules VI/VII and IX/X, is reminiscent of the gene expression heterogeneity that has been observed in Purkinje cells and other cerebellar neurons (1). Perhaps the most relevant of these expression patterns is that of the small heat shock protein HSP25, which in the adult cerebellum is selectively expressed by zones of Purkinje cells in lobules VI/VII and IX/X (17). We therefore mapped the distributions of HSP25 and *Npy-Gfp* to test the hypothesis that Bergmann glial cells might share a common molecular topography with specific subsets of Purkinje cells. Indeed, on coronal tissue sections cut through adult cerebella we observed a substantial overlap between the expression domains of *Npy-Gfp* marked Bergmann glia and HSP25 immunoreactive Purkinje cells (Fig. 4). Each zone of glial cells accompanied a specific zone of Purkinje cells. But, although the number of zones was the same for each cellular marker (5 zones in lobules VI–VII and up to 5 in lobules IX–X), the boundaries of the glial cell zones were not as sharp as the boundaries of the Purkinje cell zones (Fig. 5). This is likely because of the basic anatomy of each cell type–both cell types extend dendrites/projections in the sagittal plane (they appear "flat"

when cut coronally), but Purkinje cells have their dendritic tree much more tightly packed in the plane. Higher power imaging of a zonal boundary best illustrates this idea (arrows Fig. 5C). The lack of perfect correspondence between the two patterns also indicates the possibility that *Npy-Gfp* Bergmann glia zones spilt HSP25 zones into a finer map (Fig. 5 and Fig. 6). In addition to this idea, that zones may be separated into sub-zones, on the more global level it is interesting that here we show *Npy-Gfp* expression in Bergmann glia revealing distinct zones in lobules VI/VII and IX/X whereas in a previous study we reported zones of *Npy-Gfp* in climbing fibers mainly within lobules I–V and VIII–IX (2). Therefore, *Npy-Gfp* expression distinguishes the four transverse domains of cerebellum (1), both by its expression in specific zonal patterns and also by its restriction to particular cell types within each region. Next we wanted to determine whether the neuron-glia zonal relationship was also present during development since adult neuronal zones are derived from specific developmental zones that are referred to as clusters (20, 24, 34).

Architectural patterning of Bergmann glia mirrors the development of Purkinje cell zones

The adult pattern of Purkinje cell zones develops around gene expression transformations that can be followed during postnatal development (35–37). To test whether a spatiotemporal relationship exists between Bergmann glia and Purkinje cell patterning we double-labeled coronal cut tissue sections from multiple ages of early postnatal mice with anti-GFP and anti-HSP25 antibodies. In addition to marking adult zones, HSP25 also distinguishes parasagittal Purkinje cell clusters in the early postnatal mouse cerebellum (38). We found that neonatal *Npy-Gfp* expression in Bergmann glia spatially corresponded with HSP25 expression in Purkinje cells at postnatal day (P) 0 ($n = 5$), P2/3 ($n = 5$) and P5 ($n = 4$). At P0, *Npy-Gfp* Bergmann glia overlap with HSP25 immunopositive Purkinje cells in a crude cluster map (Fig. 6A–A″). On P2/3 coronal sections, we detected two HSP25 parasagittal clusters that are located lateral to the midline (39) (Fig. 6B). *Npy-Gfp* is also strongly expressed at P2/3 in two clusters that are located adjacent to the midline and they share the zonal boundaries that are delineated by HSP25 expression in Purkinje cells (Fig. 6B′-B″). However, like many other early onset postnatal markers, the expression boundaries are poorly defined during this stage of cerebellar ontogenesis (37, 40, 41). As shown previously, most Purkinje cells in the P5 cerebellum express HSP25 (38). We observed that *Npy-Gfp* is also widely expressed at P5, and its distribution in Bergmann glia correlated with the uniform expression of HSP25 in Purkinje cells (Fig. 6C–C″). By P10, HSP25 is expressed in Purkinje cell zones in lobules VI/VII and IX/X (Fig. 6D; (39) $n = 6$). At this stage, we observed that the pattern of *Npy-Gfp* in Bergmann glia again overlapped with zones of HSP25 expression in Purkinje cells (Fig. 6D–D″). The corresponding patterns of HSP25 and *Npy-Gfp* observed during the second week of postnatal development continued into adulthood (Fig. 4 and Fig. 6E–E″). These data suggest that the architectural patterning of Bergmann glia respects the same parasagittal zone boundaries as Purkinje cells, and their refinement into adult zones is temporally coordinated during postnatal development.

Loss of Npy does not alter the patterning of Purkinje cell zones

Npy has multiple functions including neuromodulation, neuroprotection, and neural development (42). In the cerebellum, it may influence network activity by modulating inhibitory synaptic transmission (28). Therefore, because of its functions in the developing

and adult cerebellum, we wanted to test whether Npy signaling itself is essential for zonal patterning by analyzing *Npy* loss of function mutant mice. Using an $Npy^{LacZ/+}$ knock-in allele, we first examined the genetically encoded *LacZ* reporter for expression in the brain (14) (Fig. 7A). Using X-gal histochemical reactivity to detect β-galactosidase expression we revealed intense punctate deposits in the cerebellum, where they were sparsely distributed mainly in lobules VI/VII and IX/X (white arrows Fig. 7B). This pattern of X-gal staining (inset Fig. 7B) is consistent with the expression of *Npy-Gfp* in the cell bodies of Bergmann glia (Fig. 1B and Fig. 2A). Although, some profiles may belong to Purkinje cells, which indeed is the case in the BAC transgenic mice since they have weak expression of *Npy-Gfp* in Purkinje cells (Fig. 1A). Then to determine whether Npy plays a role in zonal patterning, we analyzed $Npy^{LacZ/LacZ}$ mutants for alterations in the pattern of HSP25. $Npy^{LacZ/LacZ}$ mutants lack both functional copies of the *Npy* gene (14). We found that the expression of HSP25 was not affected by the loss of Npy signaling in the brain (Fig. 7C–D). Immunohistochemical staining revealed the same number of Purkinje cell zones in control compared to $Npy^{LacZ/LacZ}$ mutant mice (Fig. 7C–D).

Discussion

We have used BAC transgenic mice that express *Gfp* driven by the *Npy* gene regulatory region to mark and follow Bergmann glia in the developing and adult mouse cerebellum. Our data demonstrates that Bergmann glia are zonally organized and that the postnatal patterning of Bergmann glia zones develops around a similar architectural plan as Purkinje cells. We show for the first time that mammalian cerebellar neurons and glia organize according to a common topography in developing and adult zones.

Bergmann glia are patterned into a topographic map of parasagittal zones

It is well established that Purkinje cell gene and protein expression delineate parasagittal zones (1) and these zones may be fundamental for motor behavior (43–46). In contrast, the lack of glial specific markers has made it difficult to determine whether glial cells are also topographically organized in the normal cerebellum. Interestingly, 5′-nucleotidase, the first histochemical marker used to demarcate cerebellar cortical longitudinal zones (47), was thought to be expressed in Bergmann glia. However, more recent work suggests that 5′-nucleotidase expression is heavily associated with Purkinje cell synapses in addition to Bergmann glia (48). Previous work also showed that viral injection, injury, and pharmacologic stress induce a zone-like distribution of proteins in glia (49–56). Based on the exquisite cellular detail revealed by GFP labeling in *Npy-Gfp* mice (Fig. 1), we demonstrate that Bergmann glia in unaffected cerebella are indeed organized around the fundamental architectural plan that is comprised of longitudinal zones (1). Together with the previous finding that Bergmann glial cells are electrically coupled within parasagittal rows (57), our expression data raise the interesting hypothesis that functional cerebellar modules may contain Bergmann glial zones (58).

Bergmann glia patterning is spatially and temporally linked to Purkinje cell zone development

Purkinje cell zones are thought to influence the zonal patterning of all cerebellar neurons including the topographic targeting of afferent projections (1, 25, 59–61). Purkinje cells are closely associated with Bergmann glia during development as the glia provide structural support for Purkinje cell dendrite extension (8). However, it has been unclear whether Bergmann glia integrate into the developing zonal plan of the cerebellum. We have found that Bergmann glial cells organize into a pattern of zones that is strikingly similar to the pattern of HSP25 Purkinje cell gene expression domains observed during normal cerebellar development (Fig. 6). Consistent with our finding, a previous study in chick used retroviruses to label and trace clones of glial cells into parasagittal clusters in the cerebellar cortex (62). Our observation that *Npy-Gfp* radial glia are arranged in clusters as early as E15 and the findings by Lin and Cepko (62) suggest that Bergmann glia may be incorporated into zones early during cerebellar development. Moreover, Lin and Cepko (62) showed compelling evidence that multipotent progenitor cells in the cerebellar ventricular zone give rise to zonally related neurons and glia. Thus, there is a tantalizing possibility that *Npy-Gfp*-Bergmann glia and HSP25-Purkinje cell zones may be derived from a common multipotent progenitor. However, our analysis of the $Npy^{LacZ/LacZ}$ mice suggests that Npy itself is probably not essential for this particular process of brain patterning (Fig. 7). But, it could be that Npy modulates synaptic function and motor behavior in a zone dependent manner. This study raises the argument that Npy mediated interactions between Bergmann and Purkinje cells are not involved in generating the patterned cerebellar map. But, the cellular and molecular mechanisms between zones of Purkinje cells and their associated Bergmann glia could provide a critical anatomical framework for controlling zonal output function during motor behavior. In this circumstance Npy protein could contribute to the cell-to-cell signaling required for circuit function within specific zones. Moreover, because HSP25 zones are particularly resistant to Purkinje cell death in diseases that exhibit patterned degeneration (54), our data raise the intriguing hypothesis that perhaps the Bergmann glia within these zones contribute not only to central and nodular domain specific functions but also to the zonally patterned cell survival in degenerative conditions. Of likely relevance, Npy may have a neuroprotective function in the central nervous system (42).

Npy-Gfp mice are ideal for visualizing zones of neuronal and glial circuits in the cerebellum

We recently showed that *Npy-Gfp* expression in climbing fibers was restricted to lobules I–V and VIII–IX in the adult mouse cerebellum (2). We also showed that within these lobules, *Npy-Gfp* was restricted to zebrinII negative zones (2), with the termination of marked climbing fibers sharply demarcating the zonal boundaries between zebrinII and PLCβ4 zones. Here, we show that the zonal architecture of *Npy-Gfp* marked cells not only extends across all regions of the vermis, but also across different cell types with a particularly remarkable localization to zones of Bergmann glia. Interestingly, the *Npy-Gfp* zones of Bergmann glia have a major overlap with HSP25 Purkinje cell zones in lobules VI/VII and IX/X where zebrinII is uniformly expressed (1, 17, 24, 41). But it is important to note that based on the Npy^{LacZ} knock-in data (Fig. 7) and on whole brain gene expression analyses (please refer to the Allen Brain Atlas database; 26, 32), the expression of Npy is relatively

weak in the cerebellum compared to other brain regions. This is in contrast to the stronger GFP expression we observed in the transgenic mouse. Thus, the *Npy* BAC reporter expression may reflect transgene specific expression, even though it labels many of the cell types reported to endogenously express Npy. Overall however, we conclude that the patterned reporter expression in the *Npy-Gfp* transgenic mouse line is a valuable *in vivo* tool for labeling Bergmann glial zones and its robust cellular expression profile will be ideal for further studying neuronal-glial interactions in tissue, cell sorting mediated molecular analyses of glial heterogeneity, and circuit activity using GFP guided recordings in slice physiology paradigms.

Acknowledgments

This work was supported by funds from Baylor College of Medicine and Texas Children's Hospital (Houston, TX). RVS is supported by the Caroline Wiess Law Fund for Research in Molecular Medicine, a BCM IDDRC Project Development Award, and by BCM IDDRC Grant Number 5P30HD024064 from the Eunice Kennedy Shriver National Institute Of Child Health & Human Development and by Grant Number C06RR029965 from the National Center For Research Resources. The BCM IDDRC Neuropathology Core conducted some of the staining.

References

1. Apps R, Hawkes R. Cerebellar cortical organization: a one-map hypothesis. Nature reviews Neuroscience. 2009; 10(9):670–81. Epub 2009/08/21. [PubMed: 19693030]
2. Reeber SL, Loeschel CA, Franklin A, Sillitoe RV. Establishment of topographic circuit zones in the cerebellum of scrambler mutant mice. Frontiers in neural circuits. 2013; 7:122. Epub 2013/07/26. [PubMed: 23885237]
3. Reeber SL, White JJ, George-Jones NA, Sillitoe RV. Architecture and development of olivocerebellar circuit topography. Frontiers in neural circuits. 2012; 6:115. Epub 2013/01/08. [PubMed: 23293588]
4. Pinto S, Roseberry AG, Liu H, Diano S, Shanabrough M, Cai X, et al. Rapid rewiring of arcuate nucleus feeding circuits by leptin. Science. 2004; 304(5667):110–5. Epub 2004/04/06. [PubMed: 15064421]
5. Wang F, Xu Q, Wang W, Takano T, Nedergaard M. Bergmann glia modulate cerebellar Purkinje cell bistability via Ca2+-dependent K+ uptake. Proceedings of the National Academy of Sciences of the United States of America. 2012; 109(20):7911–6. Epub 2012/05/02. [PubMed: 22547829]
6. Muller T, Kettenmann H. Physiology of Bergmann glial cells. International review of neurobiology. 1995; 38:341–59. Epub 1995/01/01. [PubMed: 8537204]
7. Karadottir R, Hamilton NB, Bakiri Y, Attwell D. Spiking and nonspiking classes of oligodendrocyte precursor glia in CNS white matter. Nature neuroscience. 2008; 11(4):450–6. Epub 2008/03/04. [PubMed: 18311136]
8. Bellamy TC. Interactions between Purkinje neurones and Bergmann glia. Cerebellum. 2006; 5(2): 116–26. Epub 2006/07/05. [PubMed: 16818386]
9. Hatten ME. Expansion of CNS precursor pools: a new role for Sonic Hedgehog. Neuron. 1999; 22(1):2–3. Epub 1999/02/23. [PubMed: 10027279]
10. Li K, Leung AW, Guo Q, Yang W, Li JY. Shp2-dependent ERK signaling is essential for induction of Bergmann glia and foliation of the cerebellum. The Journal of neuroscience : the official journal of the Society for Neuroscience. 2014; 34(3):922–31. Epub 2014/01/17. [PubMed: 24431450]
11. Qiu Z, Cang Y, Goff SP. Abl family tyrosine kinases are essential for basement membrane integrity and cortical lamination in the cerebellum. The Journal of neuroscience : the official journal of the Society for Neuroscience. 2010; 30(43):14430–9. Epub 2010/10/29. [PubMed: 20980600]
12. Saab AS, Neumeyer A, Jahn HM, Cupido A, Simek AA, Boele HJ, et al. Bergmann glial AMPA receptors are required for fine motor coordination. Science. 2012; 337(6095):749–53. Epub 2012/07/07. [PubMed: 22767895]

13. Nishiyama H, Fukaya M, Watanabe M, Linden DJ. Axonal motility and its modulation by activity are branch-type specific in the intact adult cerebellum. Neuron. 2007; 56(3):472–87. Epub 2007/11/09. [PubMed: 17988631]

14. Erickson JC, Clegg KE, Palmiter RD. Sensitivity to leptin and susceptibility to seizures of mice lacking neuropeptide Y. Nature. 1996; 381(6581):415–21. Epub 1996/05/30. [PubMed: 8632796]

15. Sillitoe RV, Stephen D, Lao Z, Joyner AL. Engrailed homeobox genes determine the organization of Purkinje cell sagittal stripe gene expression in the adult cerebellum. The Journal of neuroscience : the official journal of the Society for Neuroscience. 2008; 28(47):12150–62. Epub 2008/11/21. [PubMed: 19020009]

16. Reeber SL, Gebre SA, Sillitoe RV. Fluorescence mapping of afferent topography in three dimensions. Brain structure & function. 2011; 216(3):159–69. Epub 2011/03/10. [PubMed: 21387082]

17. Armstrong CL, Krueger-Naug AM, Currie RW, Hawkes R. Constitutive expression of the 25-kDa heat shock protein Hsp25 reveals novel parasagittal bands of purkinje cells in the adult mouse cerebellar cortex. The Journal of comparative neurology. 2000; 416(3):383–97. Epub 1999/12/22. [PubMed: 10602096]

18. Bignami A, Dahl D. The development of Bergmann glia in mutant mice with cerebellar malformations: reeler, staggerer and weaver. Immunofluorescence study with antibodies to the glial fibrillary acidic protein. The Journal of comparative neurology. 1974; 155(2):219–29. Epub 1974/05/15. [PubMed: 4597104]

19. Yuasa S. Bergmann glial development in the mouse cerebellum as revealed by tenascin expression. Anatomy and embryology. 1996; 194(3):223–34. Epub 1996/09/01. [PubMed: 8849669]

20. Sillitoe RV, Gopal N, Joyner AL. Embryonic origins of ZebrinII parasagittal stripes and establishment of topographic Purkinje cell projections. Neuroscience. 2009; 162(3):574–88. Epub 2009/01/20. [PubMed: 19150487]

21. Sillitoe RV, Chung SH, Fritschy JM, Hoy M, Hawkes R. Golgi cell dendrites are restricted by Purkinje cell stripe boundaries in the adult mouse cerebellar cortex. The Journal of neuroscience : the official journal of the Society for Neuroscience. 2008; 28(11):2820–6. Epub 2008/03/14. [PubMed: 18337412]

22. Larsell O. The morphogenesis and adult pattern of the lobules and fissures of the cerebellum of the white rat. The Journal of comparative neurology. 1952; 97(2):281–356. Epub 1952/10/01. [PubMed: 12999992]

23. Larsell, O., Jansen, J. The comparative anatomy and histology of the cerebellum. Minneapolis: University of Minnesota Press; 1967.

24. Ozol K, Hayden JM, Oberdick J, Hawkes R. Transverse zones in the vermis of the mouse cerebellum. The Journal of comparative neurology. 1999; 412(1):95–111. Epub 1999/08/10. [PubMed: 10440712]

25. Sillitoe RV, Joyner AL. Morphology, molecular codes, and circuitry produce the three-dimensional complexity of the cerebellum. Annual review of cell and developmental biology. 2007; 23:549–77. Epub 2007/05/18.

26. Lein ES, Hawrylycz MJ, Ao N, Ayres M, Bensinger A, Bernard A, et al. Genome-wide atlas of gene expression in the adult mouse brain. Nature. 2007; 445(7124):168–76. Epub 2006/12/08. [PubMed: 17151600]

27. Akiyama K, Nakanishi S, Nakamura NH, Naito T. Gene expression profiling of neuropeptides in mouse cerebellum, hippocampus, and retina. Nutrition. 2008; 24(9):918–23. Epub 2008/07/30. [PubMed: 18662864]

28. Dubois CJ, Ramamoorthy P, Whim MD, Liu SJ. Activation of NPY type 5 receptors induces a long-lasting increase in spontaneous GABA release from cerebellar inhibitory interneurons. Journal of neurophysiology. 2012; 107(6):1655–65. Epub 2011/12/23. [PubMed: 22190627]

29. Liu HZ, Li XY, Tong JJ, Qiu ZY, Zhan HC, Sha JN, et al. Duck cerebellum participates in regulation of food intake via the neurotransmitters serotonin and neuropeptide Y. Nutritional neuroscience. 2008; 11(5):200–6. Epub 2008/09/11. [PubMed: 18782479]

30. Ueyama T, Houtani T, Nakagawa H, Baba K, Ikeda M, Yamashita T, et al. A subpopulation of olivocerebellar projection neurons express neuropeptide Y. Brain research. 1994; 634(2):353–7. Epub 1994/01/21. [PubMed: 8131087]

31. Morara S, Marcoti W, Provini L, Rosina A. Neuropeptide Y (NPY) expression is up-regulated in the rat inferior olive during development. Neuroreport. 1997; 8(17):3743–7. Epub 1998/01/14. [PubMed: 9427362]

32. Allen Mouse Brain Atlas. Allen Institute for Brain Science. 2014. [updated 2014; cited 2014]; Available from: http://mouse.brain-map.org/

33. Eiraku M, Tohgo A, Ono K, Kaneko M, Fujishima K, Hirano T, et al. DNER acts as a neuron-specific Notch ligand during Bergmann glial development. Nature neuroscience. 2005; 8(7):873–80. Epub 2005/06/21. [PubMed: 15965470]

34. Larouche M, Che PM, Hawkes R. Neurogranin expression identifies a novel array of Purkinje cell parasagittal stripes during mouse cerebellar development. The Journal of comparative neurology. 2006; 494(2):215–27. Epub 2005/12/02. [PubMed: 16320235]

35. Marzban H, Chung S, Watanabe M, Hawkes R. Phospholipase Cbeta4 expression reveals the continuity of cerebellar topography through development. The Journal of comparative neurology. 2007; 502(5):857–71. Epub 2007/04/17. [PubMed: 17436294]

36. Fujita H, Morita N, Furuichi T, Sugihara I. Clustered fine compartmentalization of the mouse embryonic cerebellar cortex and its rearrangement into the postnatal striped configuration. The Journal of neuroscience : the official journal of the Society for Neuroscience. 2012; 32(45):15688–703. Epub 2012/11/09. [PubMed: 23136409]

37. White JJ, Sillitoe RV. Postnatal development of cerebellar zones revealed by neurofilament heavy chain protein expression. Frontiers in neuroanatomy. 2013; 7:9. Epub 2013/05/16. [PubMed: 23675325]

38. Armstrong CL, Krueger-Naug AM, Currie RW, Hawkes R. Expression of heat-shock protein Hsp25 in mouse Purkinje cells during development reveals novel features of cerebellar compartmentation. The Journal of comparative neurology. 2001; 429(1):7–21. Epub 2000/11/22. [PubMed: 11086286]

39. Armstrong CL, Chung SH, Armstrong JN, Hochgeschwender U, Jeong YG, Hawkes R. A novel somatostatin-immunoreactive mossy fiber pathway associated with HSP25-immunoreactive purkinje cell stripes in the mouse cerebellum. The Journal of comparative neurology. 2009; 517(4): 524–38. Epub 2009/10/02. [PubMed: 19795496]

40. Larouche M, Hawkes R. From clusters to stripes: the developmental origins of adult cerebellar compartmentation. Cerebellum. 2006; 5(2):77–88. Epub 2006/07/05. [PubMed: 16818382]

41. Sillitoe, RV., Hawkes, R. Zones and Stripes: Development of Cerebellar Topography. In: Manto, M-U.Gruol, DL.Schmahmann, JD.Koibuchi, N., Rossi, F., editors. Handbook of the cerebellum and cerebellar disorders. New York [u.a.]: Springer; 2013. p. 43-59.

42. Santos-Carvalho A, Alvaro AR, Martins J, Ambrosio AF, Cavadas C. Emerging novel roles of neuropeptide Y in the retina: from neuromodulation to neuroprotection. Progress in neurobiology. 2014; 112:70–9. Epub 2013/11/05. [PubMed: 24184719]

43. Attwell PJ, Rahman S, Ivarsson M, Yeo CH. Cerebellar cortical AMPA-kainate receptor blockade prevents performance of classically conditioned nictitating membrane responses. The Journal of neuroscience : the official journal of the Society for Neuroscience. 1999; 19(24):RC45. Epub 1999/12/14. [PubMed: 10594089]

44. Schonewille M, Luo C, Ruigrok TJ, Voogd J, Schmolesky MT, Rutteman M, et al. Zonal organization of the mouse flocculus: physiology, input, and output. The Journal of comparative neurology. 2006; 497(4):670–82. Epub 2006/06/02. [PubMed: 16739198]

45. Horn KM, Pong M, Gibson AR. Functional relations of cerebellar modules of the cat. The Journal of neuroscience : the official journal of the Society for Neuroscience. 2010; 30(28):9411–23. Epub 2010/07/16. [PubMed: 20631170]

46. Mostofi A, Holtzman T, Grout AS, Yeo CH, Edgley SA. Electrophysiological localization of eyeblink-related microzones in rabbit cerebellar cortex. The Journal of neuroscience : the official journal of the Society for Neuroscience. 2010; 30(26):8920–34. Epub 2010/07/02. [PubMed: 20592214]

47. Scott TG. A Unique Pattern of Localization within the Cerebellum. Nature. 1963; 200:793. Epub 1963/11/23.
48. Bailly Y, Schoen SW, Delhaye-Bouchaud N, Kreutzberg GW, Mariani J. 5′-nucleotidase activity as a synaptic marker of parasagittal compartmentation in the mouse cerebellum. Journal of neurocytology. 1995; 24(11):879–90. Epub 1995/11/01. [PubMed: 8576716]
49. O'Hearn E, Molliver ME. Degeneration of Purkinje cells in parasagittal zones of the cerebellar vermis after treatment with ibogaine or harmaline. Neuroscience. 1993; 55(2):303–10. Epub 1993/07/01. [PubMed: 8377927]
50. Nakki R, Koistinaho J, Sharp FR, Sagar SM. Cerebellar toxicity of phencyclidine. J Neurosci. 1995; 15(3 Pt 2):2097–108. Epub 1995/03/01. [PubMed: 7891155]
51. Fukuda K, Aihara N, Sagar SM, Sharp FR, Pitts LH, Honkaniemi J, et al. Purkinje cell vulnerability to mild traumatic brain injury. J Neurotrauma. 1996; 13(5):255–66. Epub 1996/05/01. [PubMed: 8797175]
52. Mautes AE, Fukuda K, Noble LJ. Cellular response in the cerebellum after midline traumatic brain injury in the rat. Neurosci Lett. 1996; 214(2–3):95–8. Epub 1996/08/23. [PubMed: 8878092]
53. O'Hearn E, Molliver ME. The olivocerebellar projection mediates ibogaine-induced degeneration of Purkinje cells: a model of indirect, trans-synaptic excitotoxicity. J Neurosci. 1997; 17(22):8828–41. Epub 1997/11/14. [PubMed: 9348351]
54. Sarna JR, Hawkes R. Patterned Purkinje cell death in the cerebellum. Prog Neurobiol. 2003; 70(6): 473–507. Epub 2003/10/22. [PubMed: 14568361]
55. Williams BL, Yaddanapudi K, Hornig M, Lipkin WI. Spatiotemporal analysis of purkinje cell degeneration relative to parasagittal expression domains in a model of neonatal viral infection. J Virol. 2007; 81(6):2675–87. Epub 2006/12/22. [PubMed: 17182680]
56. Igarashi T, Potts MB, Noble-Haeusslein LJ. Injury severity determines Purkinje cell loss and microglial activation in the cerebellum after cortical contusion injury. Exp Neurol. 2007; 203(1): 258–68. Epub 2006/10/19. [PubMed: 17045589]
57. Muller T, Moller T, Neuhaus J, Kettenmann H. Electrical coupling among Bergmann glial cells and its modulation by glutamate receptor activation. Glia. 1996; 17(4):274–84. Epub 1996/08/01. [PubMed: 8856324]
58. Ruigrok TJ. Ins and outs of cerebellar modules. Cerebellum. 2011; 10(3):464–74. Epub 2010/03/17. [PubMed: 20232190]
59. Sotelo C. Cellular and genetic regulation of the development of the cerebellar system. Progress in neurobiology. 2004; 72(5):295–339. Epub 2004/05/26. [PubMed: 15157725]
60. Sotelo C, Chedotal A. Development of the olivocerebellar system: migration and formation of cerebellar maps. Progress in brain research. 2005; 148:1–20. Epub 2005/01/22. [PubMed: 15661177]
61. Sillitoe RV, Vogel MW, Joyner AL. Engrailed homeobox genes regulate establishment of the cerebellar afferent circuit map. The Journal of neuroscience : the official journal of the Society for Neuroscience. 2010; 30(30):10015–24. Epub 2010/07/30. [PubMed: 20668186]
62. Lin JC, Cepko CL. Biphasic dispersion of clones containing Purkinje cells and glia in the developing chick cerebellum. Developmental biology. 1999; 211(2):177–97. Epub 1999/07/09. [PubMed: 10395781]
63. Armstrong CL, Hawkes R. Pattern formation in the cerebellar cortex. Biochemistry and cell biology = Biochimie et biologie cellulaire. 2000; 78(5):551–62. Epub 2000/12/05. [PubMed: 11103945]

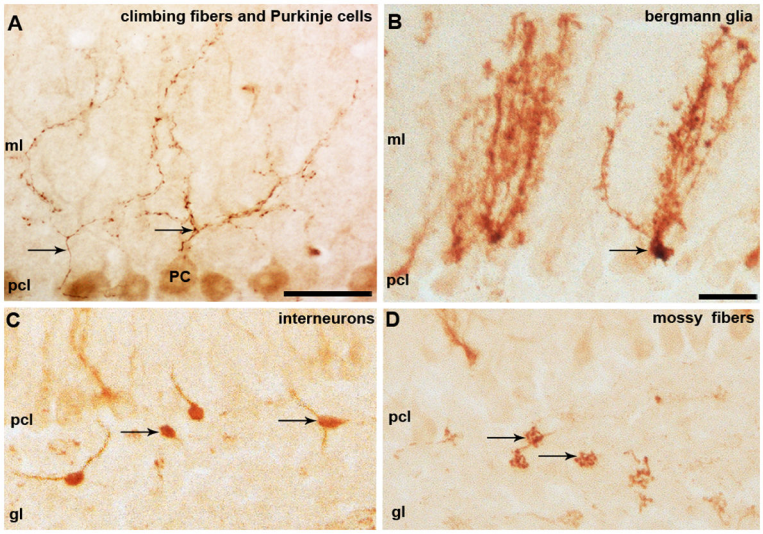

Figure 1.

Npy-Gfp is expressed in cerebellar neurons, afferent fibers, and glia. **A**. *Npy-Gfp* is expressed in climbing fibers (arrows) and Purkinje cells (PC). **B**. *Npy-Gfp* is heavily expressed in Bergmann glial cells that are intermingled between Purkinje cells. **C**. Golgi cells and other granular layer interneurons were labeled by *Npy-Gfp* (arrows). **D**. High magnification image of *Npy-Gfp* labeled mossy fibers and their large terminal rosettes (arrows) in the granular layer. Abbreviations: molecular layer (ml); Purkinje cell layer (plc); granular layer (gl). Scale bars in **A** and **B** = 20 μm; in **B** applies to **B**–**D**).

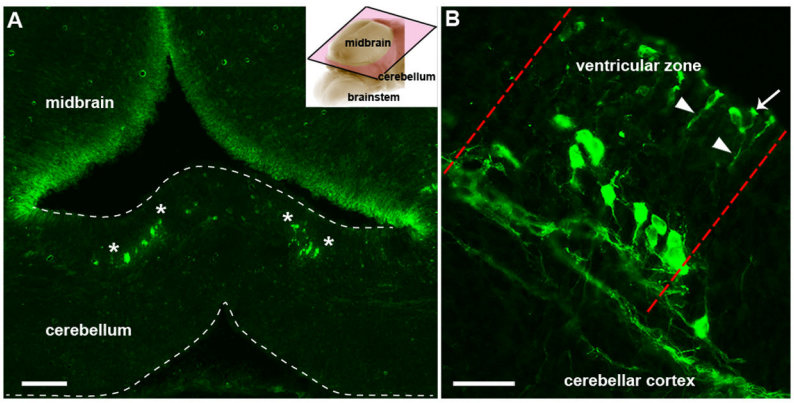

Figure 2.

Npy-Gfp labeled radial glia are arranged into clusters in the cerebellum of E15 embryos. **A**. Coronal sections cut through an E15 cerebellum showing clusters of *Npy-Gfp* immunoreactive radial glia arranged symmetrically about the midline (their boundaries are delineated by the white asterisks). Inset in (**A)** demonstrates the planar cut (pink frame outlined with black trim) of the tissue section in **A** and **B. B**. Higher magnification image illustrating *Npy-Gfp* expression in a radial glia cluster (the lateral limits are indicated by the red dotted lines) in the ventricular zone and showing the long radial fibers (arrowheads) with endfeet that project to the ventricular surface of the cerebellum (arrow). Scale bar in **A** = 100 μm; in **B** = 30 μm.

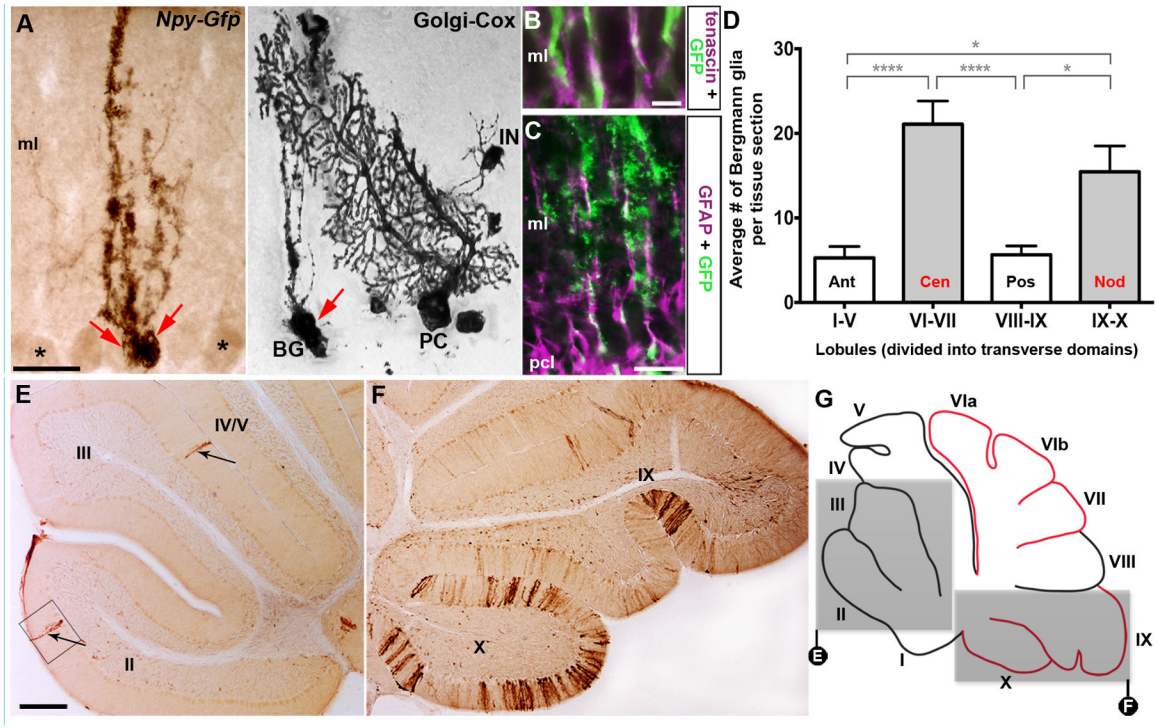

Figure 3.

Npy-Gfp labeled Bergmann glia are spatially organized in the cerebellum. **A**. High magnification image of an *Npy-Gfp* labeled Bergmann glial cell in the Purkinje cell layer of the mouse cerebellum. Golgi-Cox labeled cerebellum showing the structure of the Bergmann glia. For comparison, note the stained Purkinje cell (PC) and interneuron (IN). Each red arrow is pointing to a Bergmann glia cell body. The asterisks mark weakly stained Purkinje cells. **B**, **C**. GFAP and tenascin co-label a subpopulation of *Npy-Gfp* labeled Bergmann glia. **D**. Quantification of the average number of Bergmann glia in each cerebellar transverse domain (error bars indicate SEM). The asterisks in **D** indicate significant differences between domains ($P < 0.05$ (*); $P < 0.0001$ (****)). *Npy-Gfp* expression in Bergmann glia is highly localized to VI–VII and IX–X. There was no significant difference in the number of marked cells between the anterior compared to the posterior domain or between the central compared to the nodular domain. **E**, **F**. GFP immunohistochemistry demonstrating the limited number of GFP marked cells in the anterior lobules compared to the large number of marked cells in the most posterior lobules. The box in E shows the Bergmann glial cell that was imaged at higher power in panel **A** and the black arrows are pointing to the processes of marked Bergmann glia. **G**. Schematic illustrating the distribution of *Npy-Gfp* expression in Bergmann glia in the adult cerebellum. The grey boxes highlight the regions captured in **E**, **F**. Anterior domain (ant; lobules 1–V), central domain (cen; lobules VI–VII), posterior domain (pos; lobules VIII– dorsal IX), and nodular domain (nod; lobules ventral IX– X). Abbreviations: ml = molecular layer; pcl = Purkinje cell layer. Scale bar in **A** and **B** = 20 μm; in **C** = 40 μm; in **E** = 250 μm (applies to E and F).

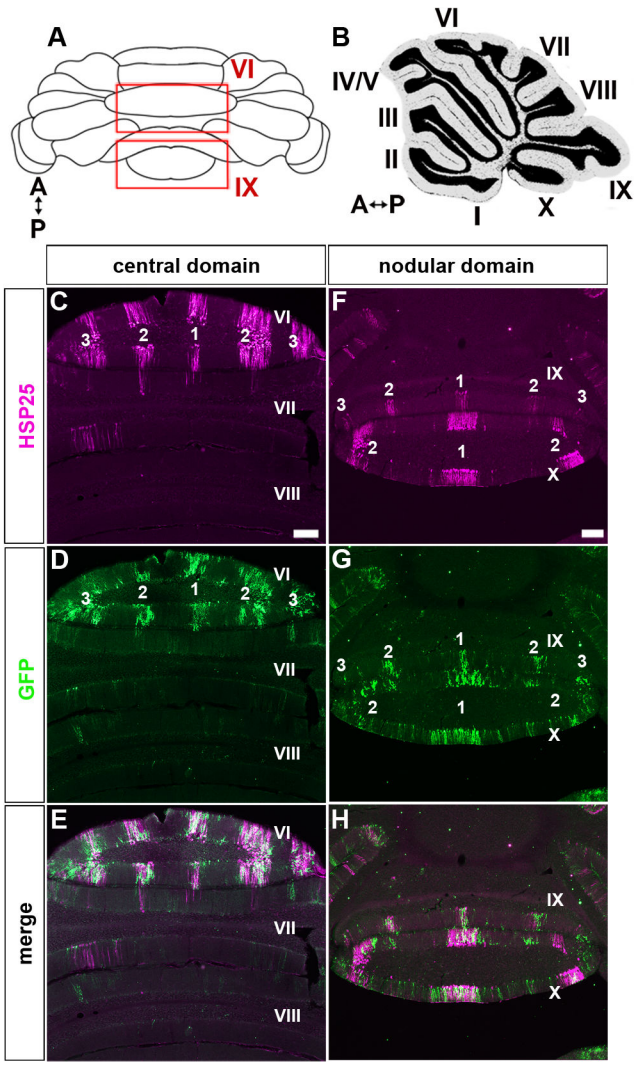

Figure 4.

Npy-Gfp expressing Bergmann glia zones overlap with HSP25 immunoreactive Purkinje cell zones. **A**. Schematic diagram of the cerebellum shown in wholemount. For the coordinates on the compass A = anterior and P = posterior (also applies to B). **B**. Sagittal schematic of the cerebellum. **C**, **D**, **E**. HSP25 and *Npy-Gfp* mark the same cerebellar zones in the central domain. The zones are labeled as 1, 2, and 3 according to a previously used HSP25 nomenclature (63). **F**, **G**, **H**. HSP25 and GFP are co-expressed in the same zones in the nodular domain. Note that the *Npy-Gfp* climbing fiber zones are not observed at these levels because they are restricted to lobules I–V and VIII-anterior IX (2) and higher magnification views are typically required to visualize the other *Npy-Gfp* marked profiles such as Purkinje cells and mossy fiber terminals (see Fig. 1). In all panels the lobules are numbered with Roman numerals. Scale bar = 100 μm in **C** (applies to D and E) and 250 μm in **F** (applies to G and H).

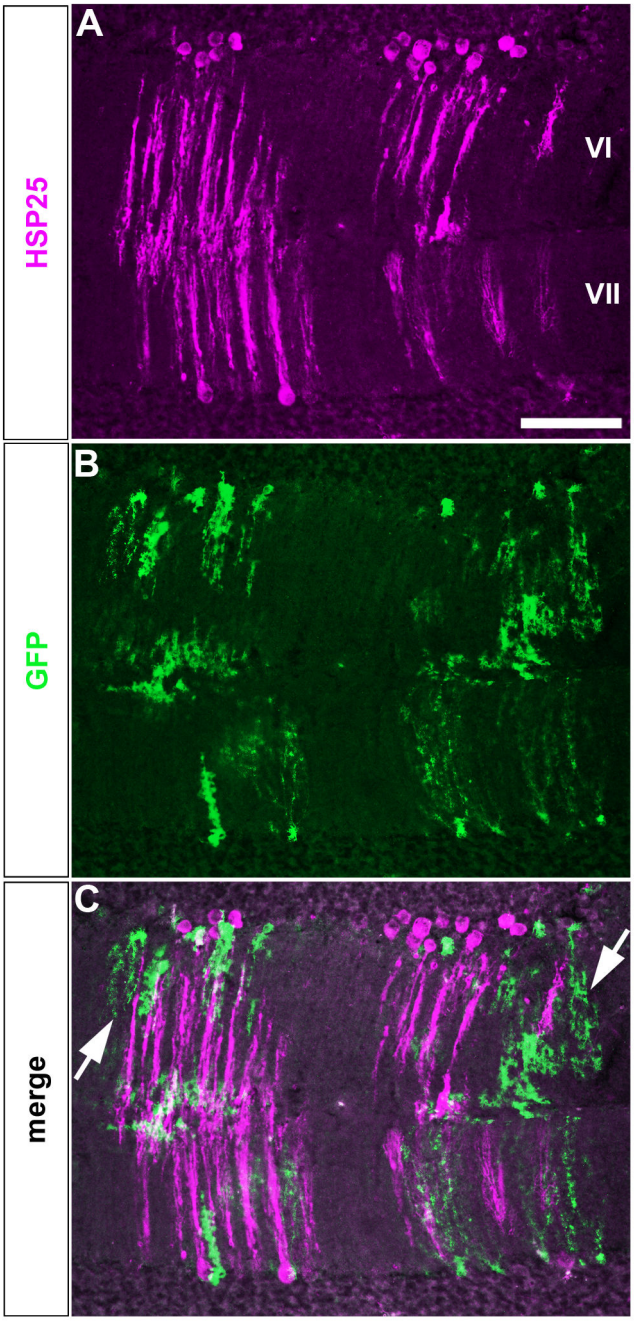

Figure 5.

The boundaries of *Npy-Gfp* Bergmann glia zones are not as sharp as HSP25 Purkinje cell zone boundaries. **A**. HSP25 immunoreactive zones in lobules VI–VII. **B**. *Npy-Gfp* marked zones in the same lobules. **C**. Merged image of the two expression patterns. Despite the overlap in each zone, the boundaries of the GFP tagged Bergmann glia are poorly defined, in part because of the orientation of the Bergmann glia (white arrows). The glial processes are not as tightly packed in the sagittal plane as the Purkinje cell dendrites. Scale bar = 75 μm in **A**.

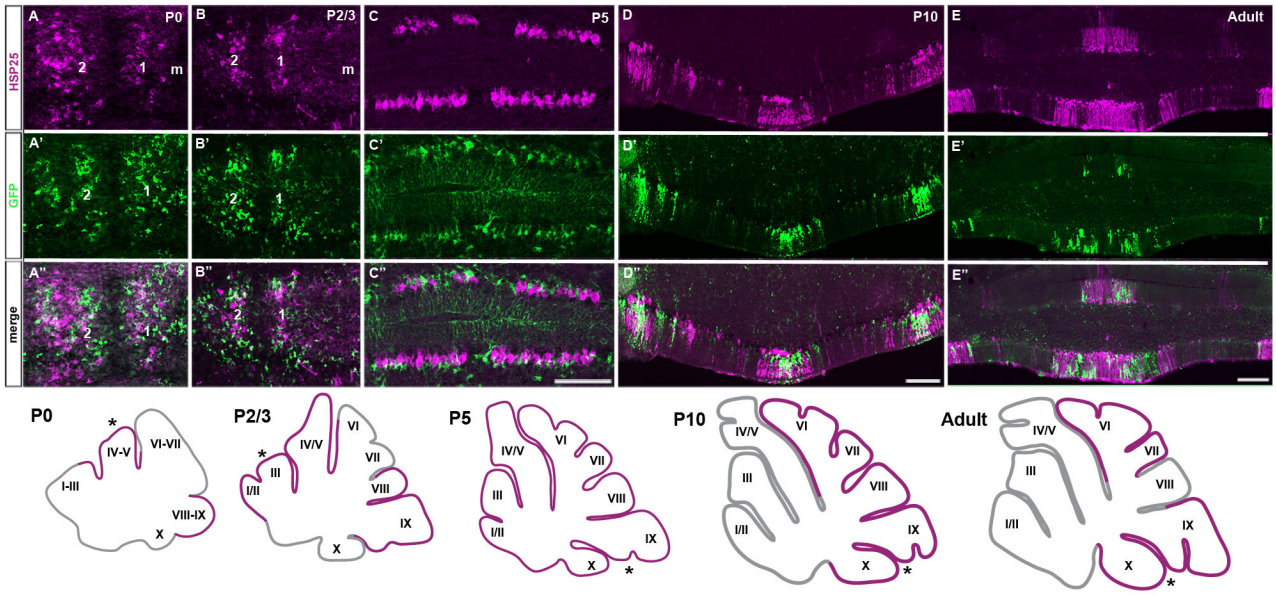

Figure 6.

Bergmann glia patterning corresponds with the development of Purkinje cell clusters. **A**. An anterior section of the mouse cerebellum at P0 revealing two distinct clusters of HSP25 immunoreactive Purkinje cells arranged symmetrically on either side of the midline (zone 1 and 2). **A′**. *Npy-Gfp* is expressed in clusters at P0, although each cluster is poorly resolved. **A″**. Merged image of panels **A** and **B** illustrating that *Npy-Gfp* Bergmann glia clusters overlap with HSP25 immunopositive Purkinje cell clusters. **B**, **B′**. An anterior section taken from a P2/3 mouse showing two lateral HSP25 (**B**) and *Npy-Gfp* (**B′**) parasagittal clusters (zone 1 and 2). **B″**. *Npy-Gfp* clusters respect HSP25 immunoreactive Purkinje cell zones. **C**, **C′**. At P5 HSP25 is expressed by the majority of Purkinje cells and *Npy-Gfp* is widely expressed in Bergmann glia. **C″**. The distribution of *Npy-Gfp* labeled Bergmann glia correlates with the uniform distribution of HSP25 immunoreactive Purkinje cells at P5. **D**, **E**. HSP25 is expressed in obvious Purkinje cell zones in the CZ and NZ at P10 (**D**) and adult (E; for clarity only lobule X is shown). **D′**, **E′**. *Npy-Gfp* is expressed in Bergmann glia zones. **D″**, **E″**. Merged images illustrating that the expression pattern of HSP25 in Purkinje cells and *Npy-Gfp* in Bergmann glia respect the same gene expression boundaries at P10 (**D″**) and in the adult cerebellum (**E″**). The schematics illustrate regions of striped HSP25 expression throughout development (38). The asterisks in the schematics indicate roughly the regions of the cerebellum where the tissue sections were taken from. Scale bar in **C″** = 200 μm (applies to **A**–**C″**); in **D″** = 200 μm (applies to **D**–**D″**; in **E″** = 250 μm (also applies to **E**–**E″**).

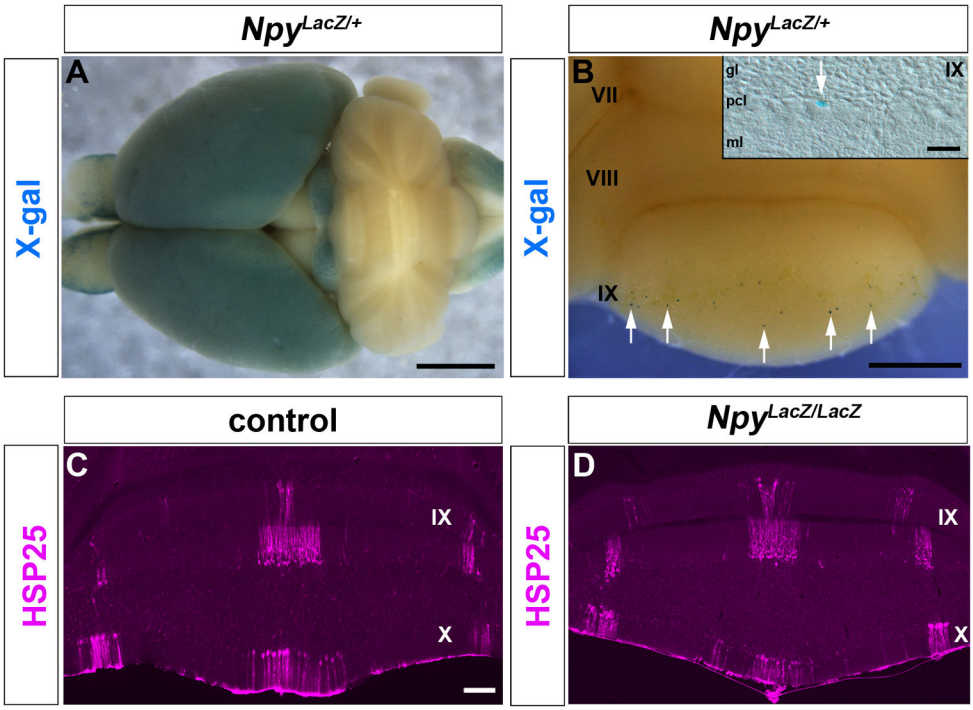

Figure 7.

Loss of the *Npy* gene does not disrupt Purkinje cell patterning. **A**. An $Npy^{LacZ/+}$ heterozygous brain stained in wholemount for X-gal histochemistry. **B**. Higher power view of the cerebellum showing the sparse punctate X-gal staining (blue reaction product). The arrows are pointing to labeled profiles that are consistent with the marking of Bergmann glial cells in the *Npy-Gfp* transgene. Some profiles are likely to be Purkinje cells. The inset shows a putative Bergmann glial cell (white arrow) wedged between Purkinje cells on a tissue section that was cut through the posterior aspect of lobule IX after wholemount X-gal staining. **C**, **D**. Similar to control mice (C), $Npy^{LacZ/LacZ}$ mutant mice that lack both copies of the *Npy* gene exhibited a clear-cut pattern of HSP25 Purkinje cell zones (D). The lobules are numbered with Roman numerals. Scale bar = 2 mm in **A**, 500 μm in **B** (20μm in the inset), and 100 μm in **C** (also applies to D).